Analysis of biologically and therapeutically relevant di- and trinucleotide analogs by tandem mass spectrometry

Dmitry Zhilyaev[2,#] Dominika Strzelecka[1,#] Sebastian Golojuch[2,3], Andrei Pandiurin[1], Jacek Jemielity[2], Joanna Kowalska[1*]

[1]Division of Biophysics, Institute of Experimental Physics, Faculty of Physics, University of Warsaw, Pasteura 5, 02-093 Warsaw, Poland

[2]Centre of New Technologies, University of Warsaw, Banacha 2c, 02-097 Warsaw, Poland

[3]Department of Chemistry, Chemistry Research Laboratory, University of Oxford, 12 Mansfield Road, Oxford OX1 3TA, UK

[#]These authors contributed equally to the manuscript

*E-mail: jkowalska@fuw.edu.pl

Supplementary Information

Figure S1. Positional [^{18}O] isotope-labeling analysis of m^{7}GpppG fragmentation by ESI(-) MS/MS. Comparison of the MS/MS spectra of **a,** unlabeled m^{7}GpppG, **b,** m^{7}Gp[^{18}O]ppG, **c,** m^{7}Gpp[^{18}O]pG, and **d,** m^{7}Gppp[^{18}O]G.

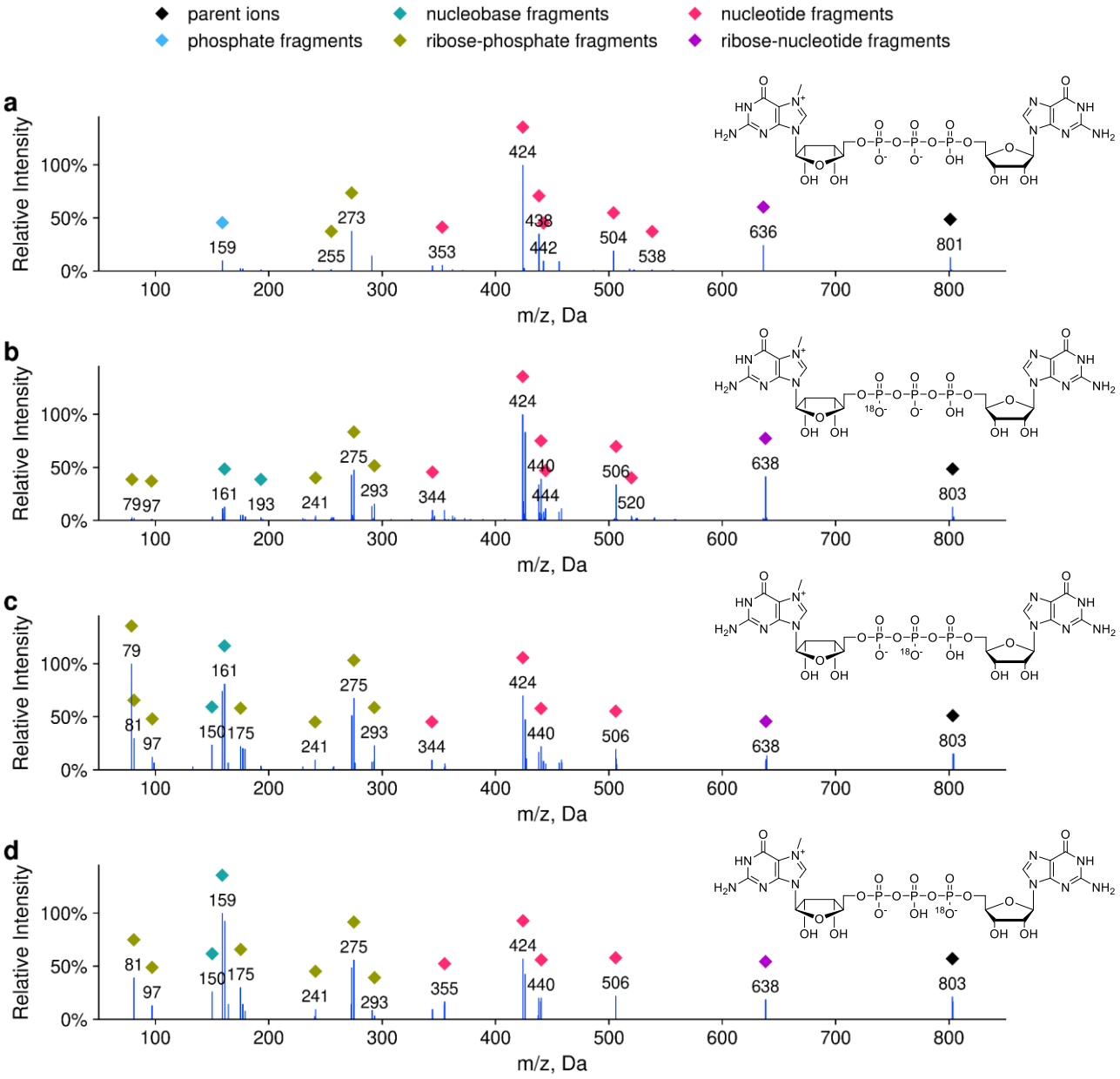


Figure S2. Negative-ion ESI-MS/MS spectra of dinucleotides with different nucleobase compositions. Comparison of spectra of doubly charged precursor ions (*z* = 2) of **a,** ApppA, **b,** ApppU, and **c,** ApppG, with selected nucleobase- and nucleotide-derived fragment ions annotated.

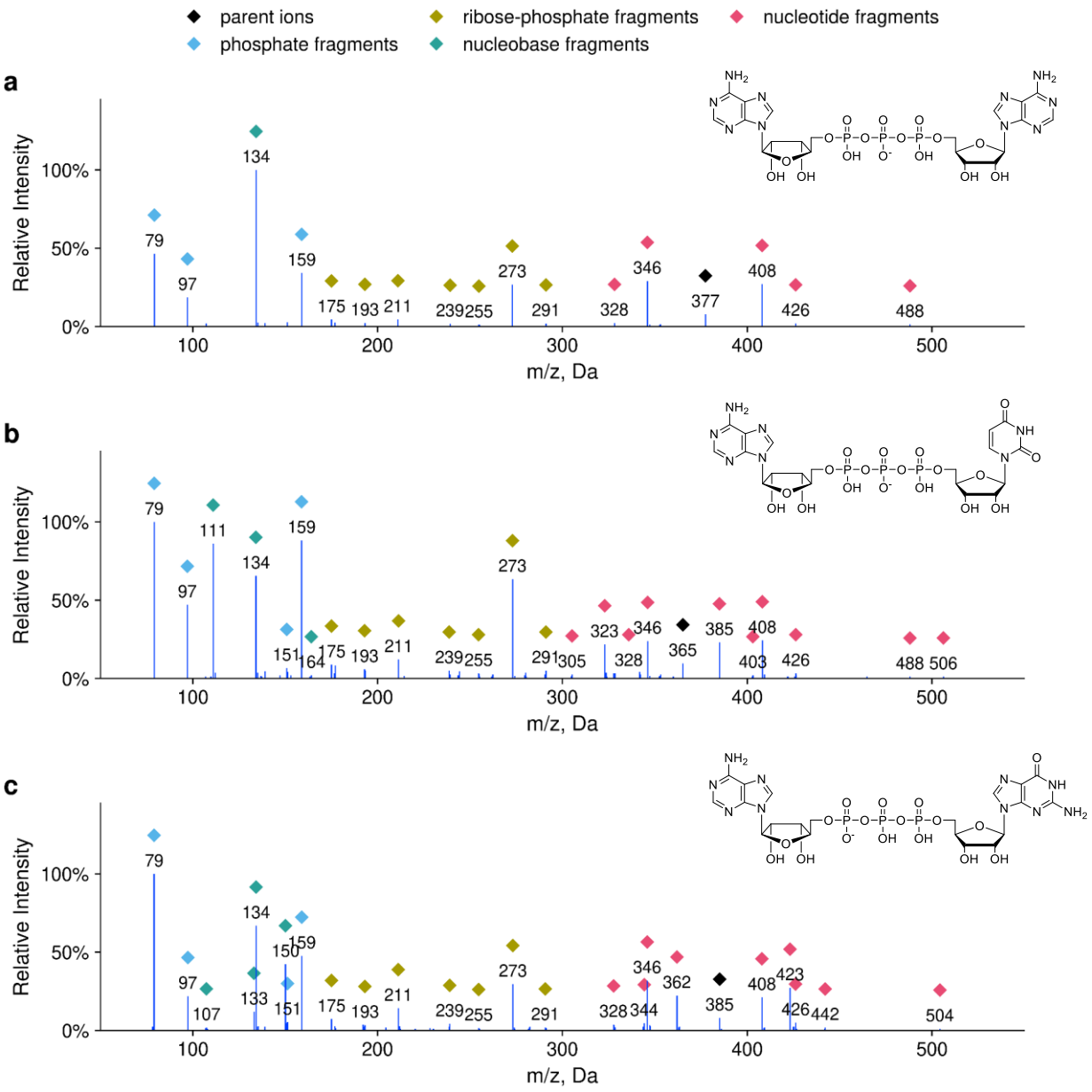


Figure S3. ESI(-) MS/MS spectra of doubly charged dinucleotides (z = 2) containing phosphate-bridge methylene modifications. Comparison of **a,** AppCH$_2$pU and **b,** ApCH$_2$ppU containing a methylene group at the 2,3- and 1,2- position of the triphosphate bridge, respectively.

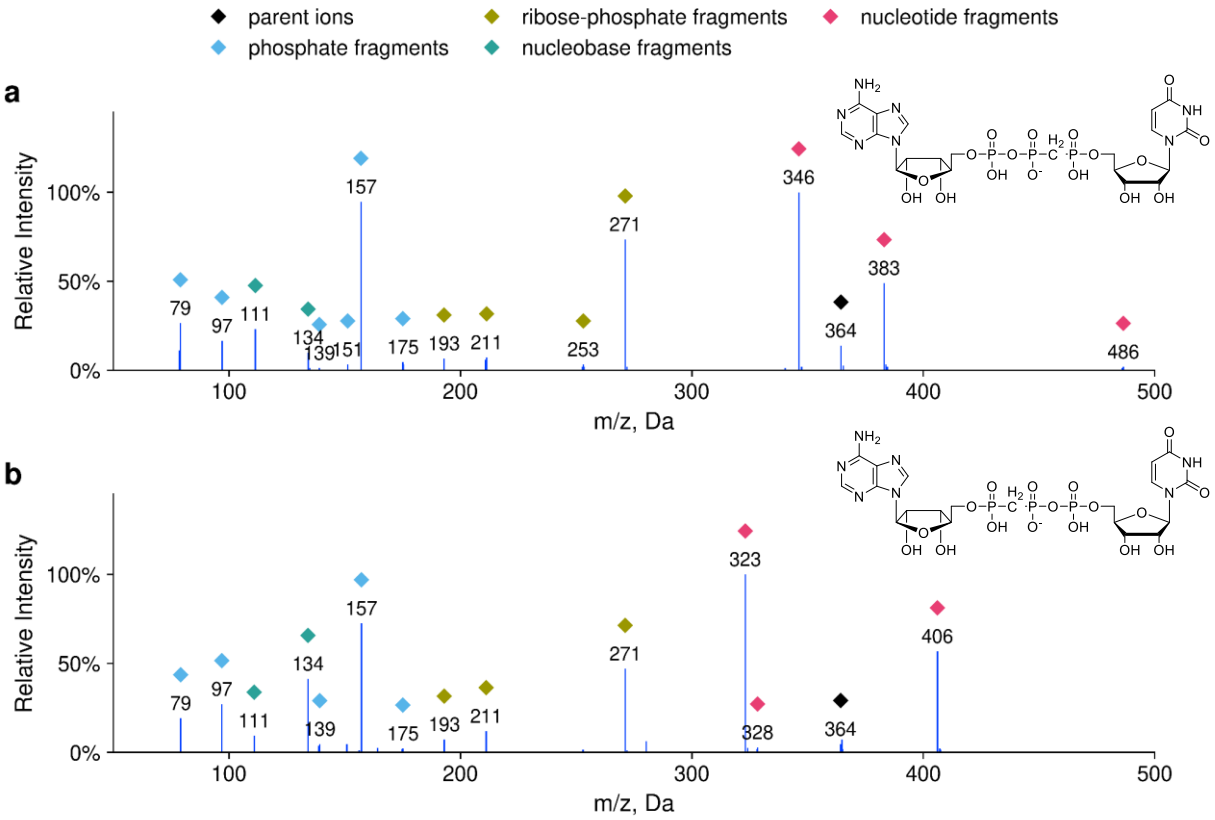


Figure S4. Negative-ion ESI-MS/MS spectra acquired at different collision energies. Doubly charged precursor ions; DP = -30 V. Panels: **a,** ApppU, CE = -25 V. **b,** AppCH$_2$pU, CE = -25 V. **c,** ApCH$_2$ppU, CE = -25 V. **d,** ApppU, CE = -30 V. **e,** AppCH$_2$pU, CE = -30 V. **f,** ApCH$_2$ppU, CE = -30 V. **g,** ApppU, CE = -35 V. **h,** AppCH$_2$pU, CE = -35 V. **i,** ApCH$_2$ppU, CE = -35 V. Intensities are normalized to the base peak in each spectrum.

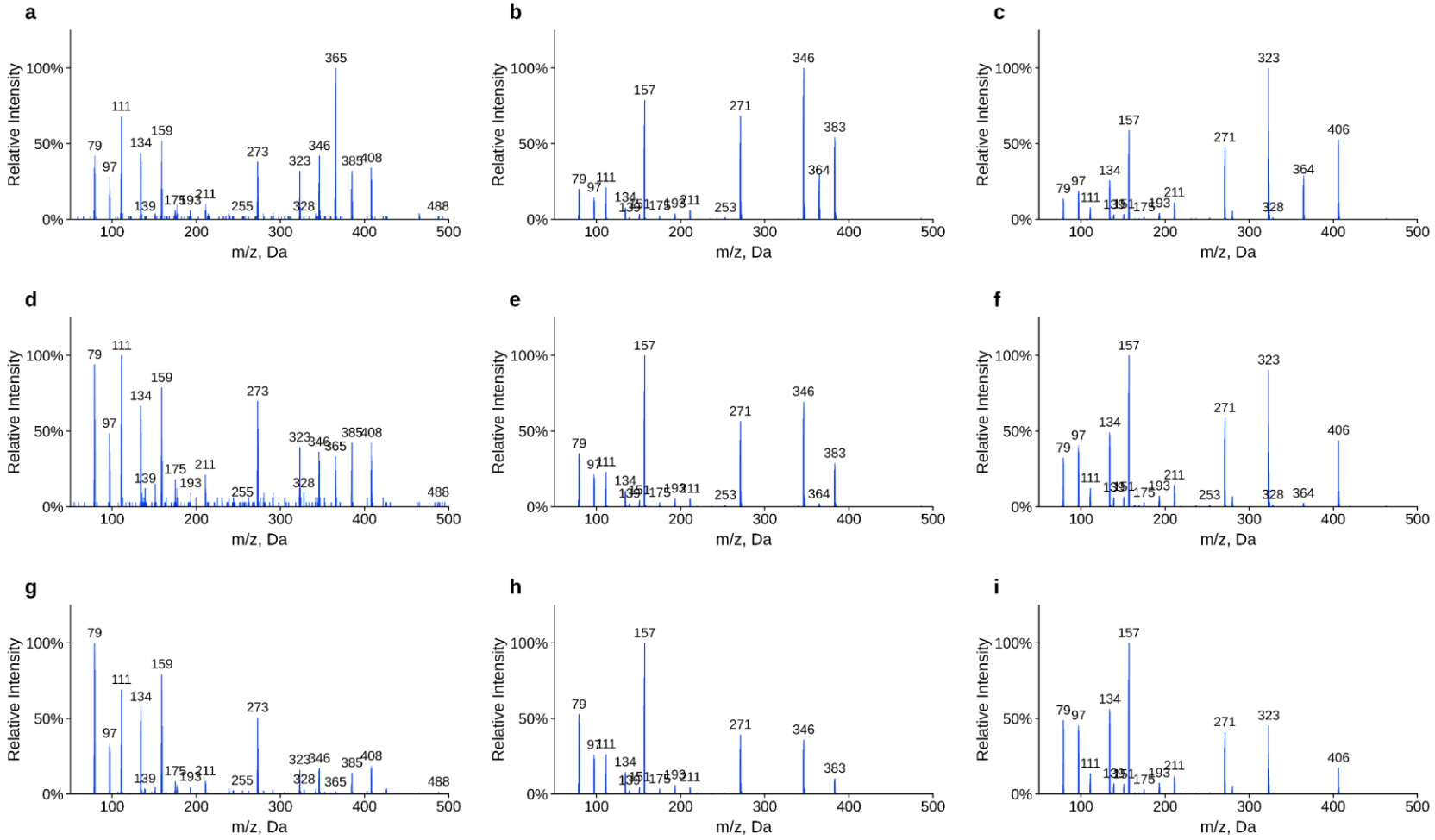


Figure S5. Negative-ion ESI-MS/MS spectra acquired at different collision energies. Singly charged precursor ions; DP = -30 V. Panels: **a,** $ApCH_2ppU$, CE = -25 V. **b,** $AppCH_2pU$, CE = -25 V. **c,** $ApCH_2ppU$, CE = -30 V. **d,** $AppCH_2pU$, CE = -30 V. **e,** $ApCH_2ppU$, CE = -35 V. **f,** $AppCH_2pU$, CE = -35 V. **g,** $ApCH_2ppU$, CE = -40 V. **h,** $AppCH_2pU$, CE = -40 V Intensities are normalized to the base peak in each spectrum.

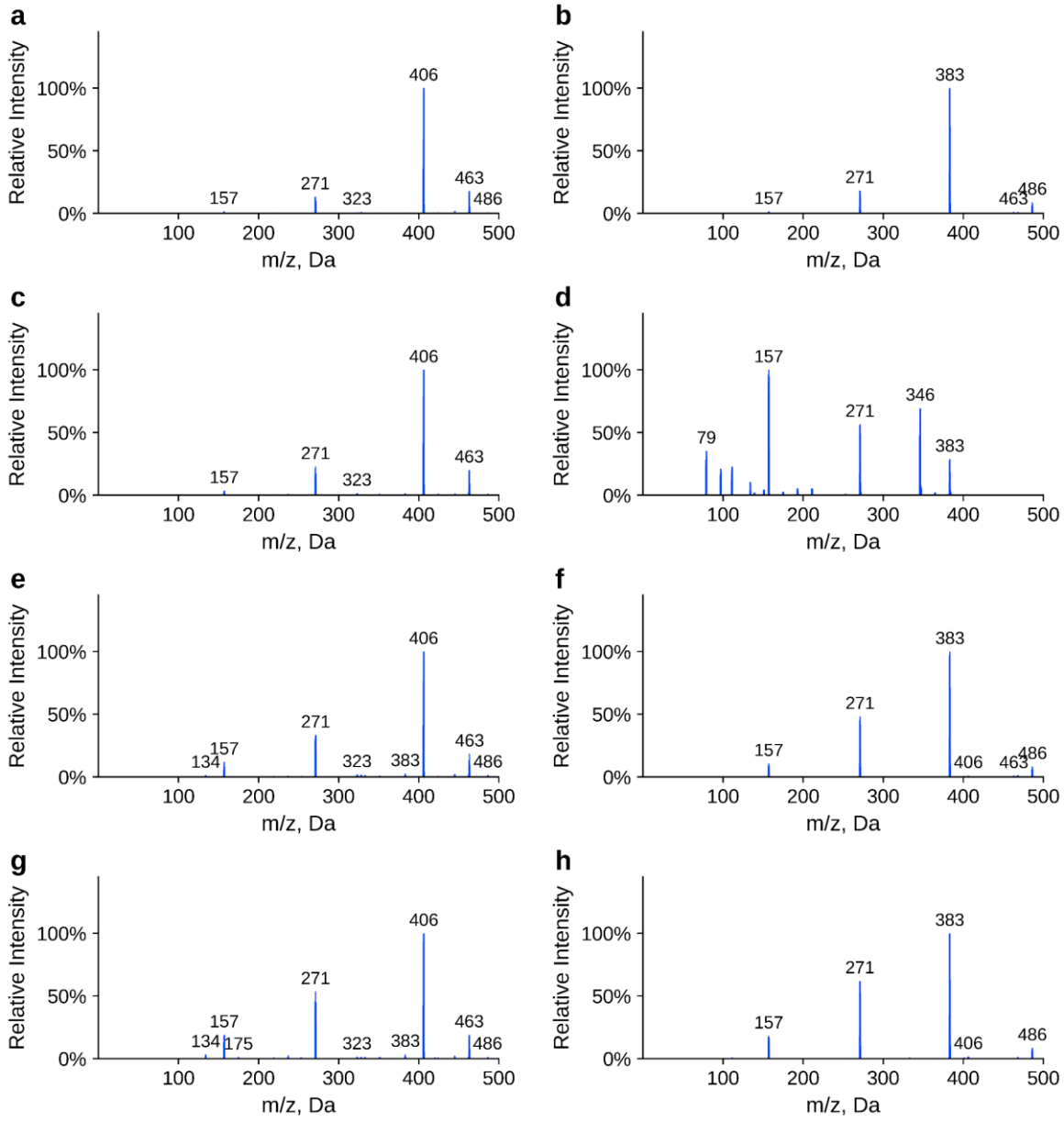


Figure S6. Negative-ion ESI-MS/MS spectra of di- and trinucleotide cap analogs. **a**, m^7GpppA. **b**, m^7GpppApG. Representative spectra showing phosphate-, ribose-phosphate-, nucleotide-, ribose-nucleotide-, dinucleotide-, and ribose-dinucleotide-derived fragment ions.

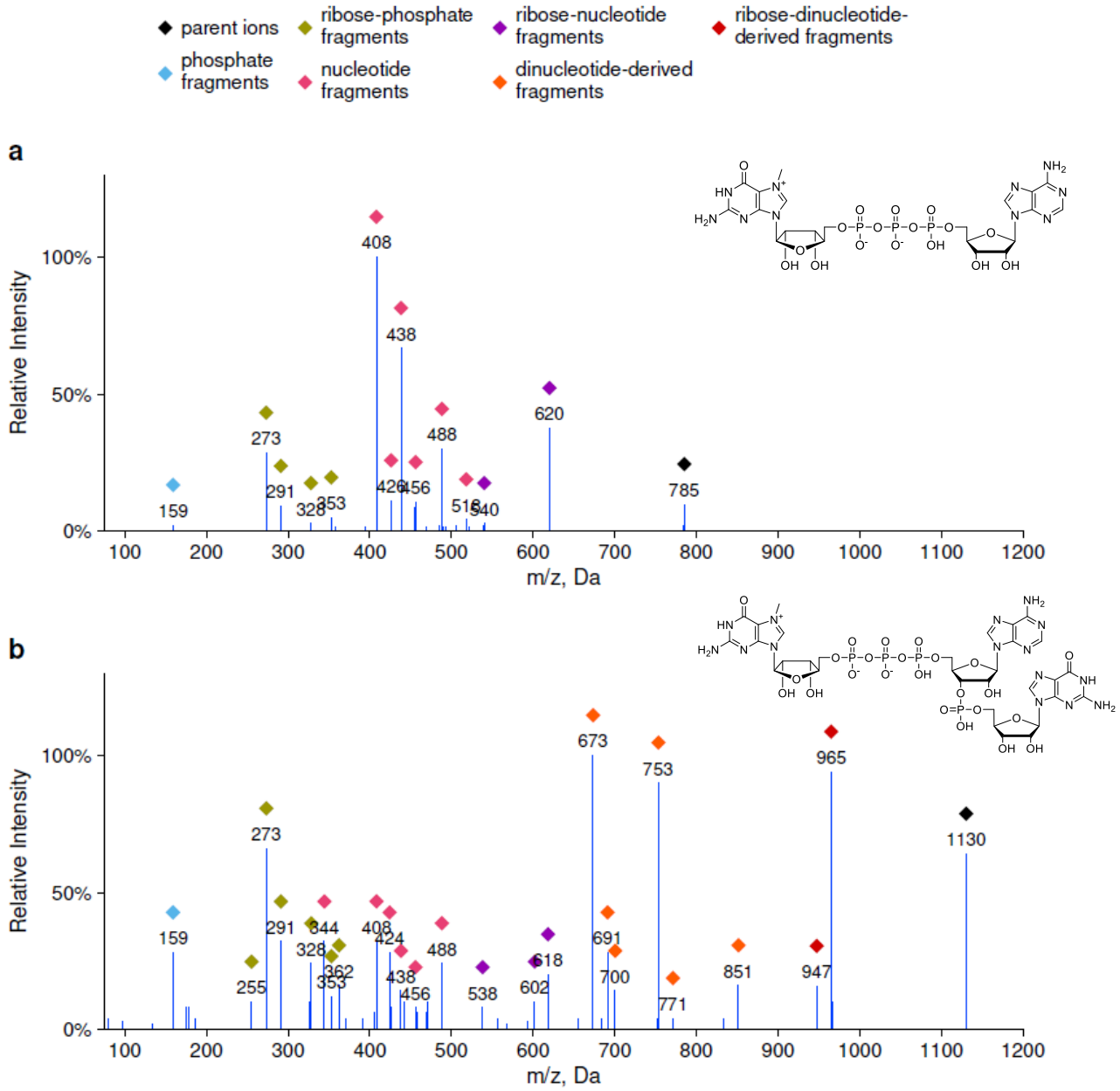


Figure S7. ESI(-) MS/MS fragmentation of trinucleotides containing a 2′-ribose modification. Comparison of the fragment-ion series observed for **a,** NADpG and its 2′-fluoro-substituted analogue **b,** NAD(F)pG, including nucleotide-, dinucleotide- and ribose-dinucleotide-derived ions.

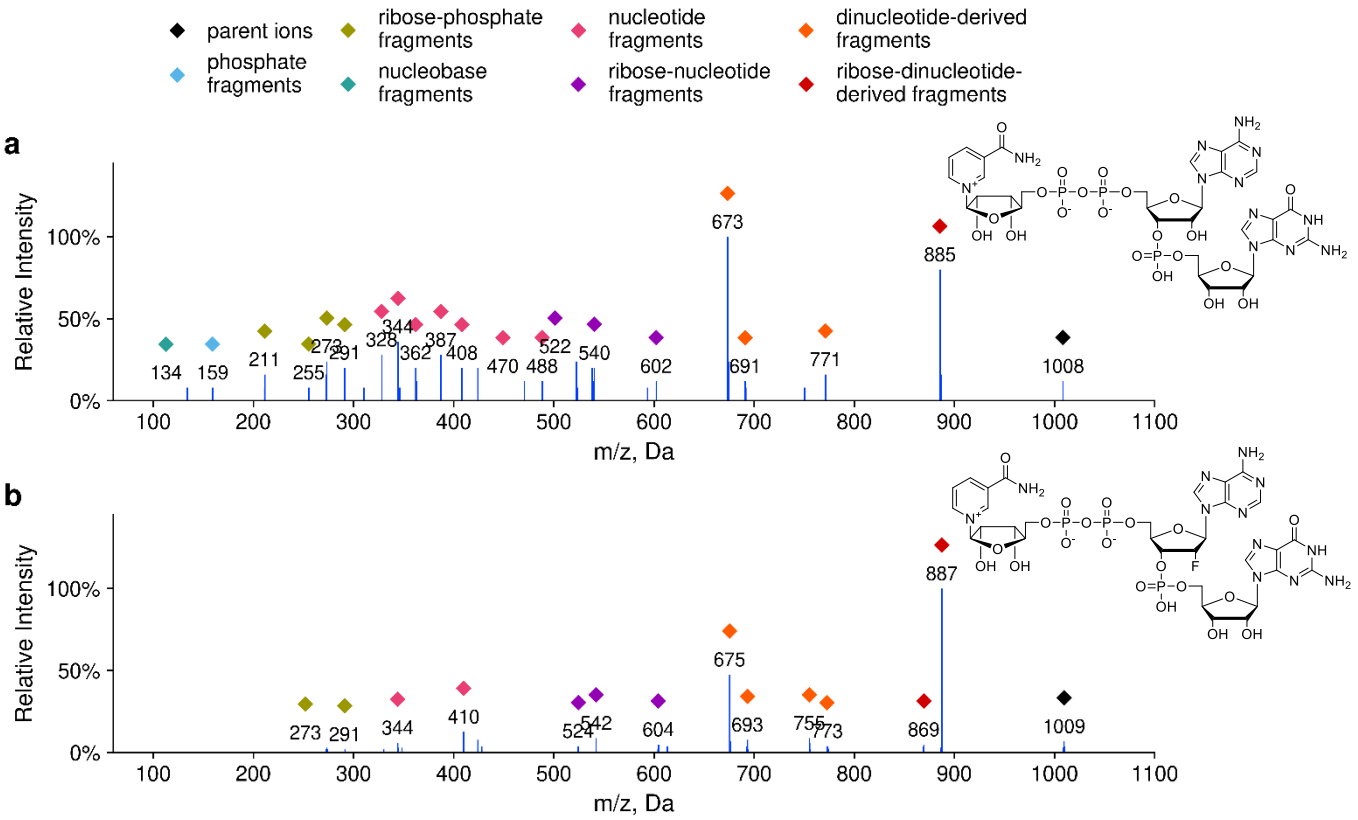


Figure S8. Negative-ion ESI-MS/MS spectra of singly charged precursor ions of isomeric mRNA cap analogs. Comparison of **a**, Cap 2 ($m^7GpppA_mpA_mpG$) and **b**, m^6A-Cap 1 ($m^7Gpppm^6A_mpApG$), showing characteristic fragmentation patterns distinguishing the two methylation isomers.

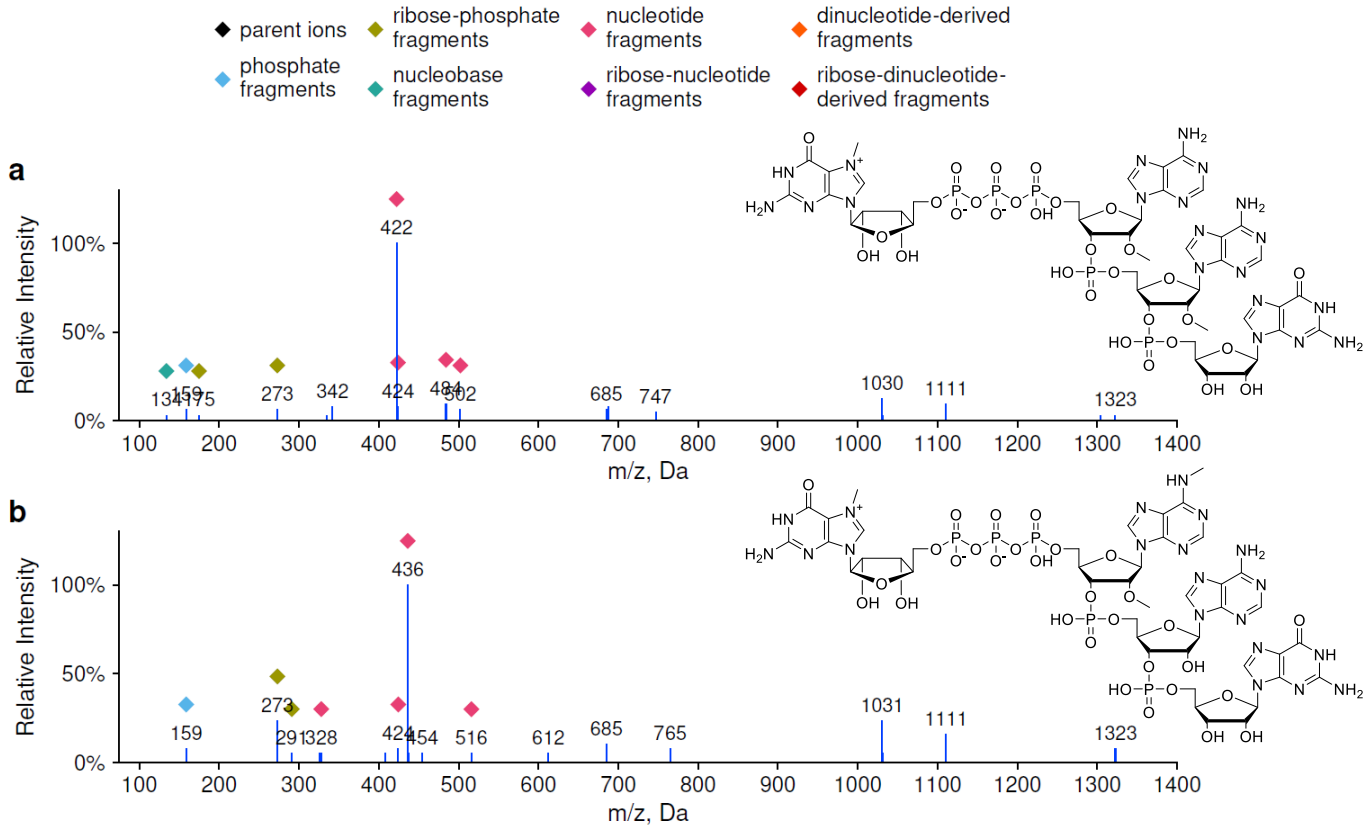
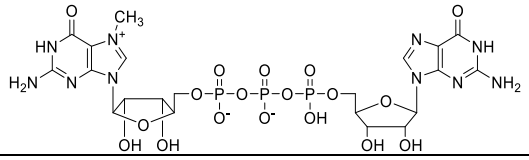
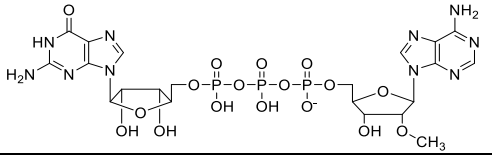
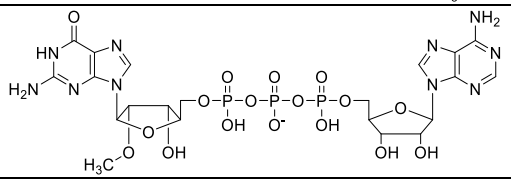
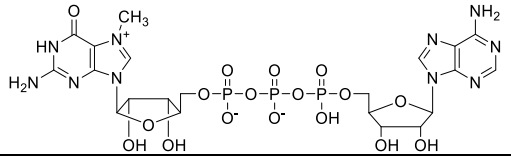
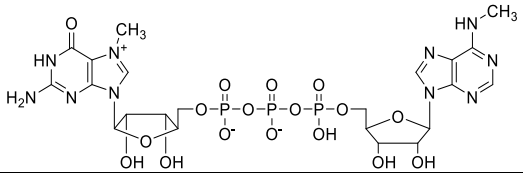
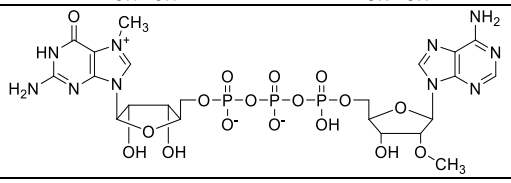
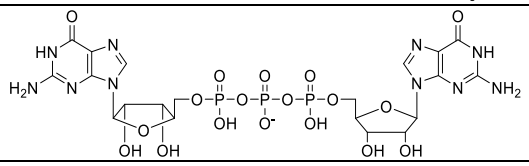
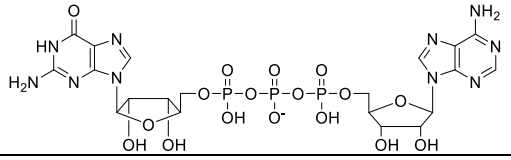
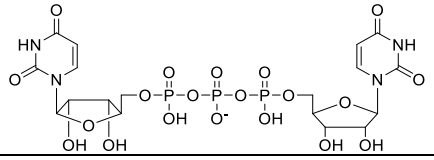
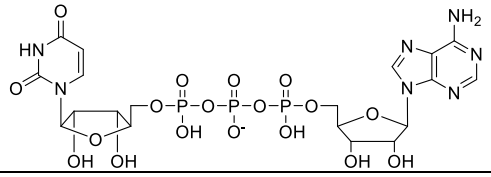
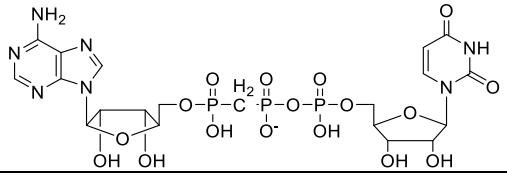
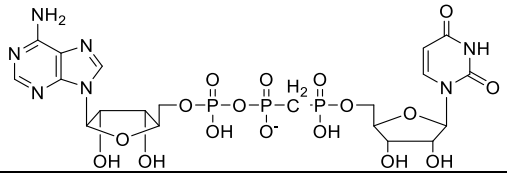
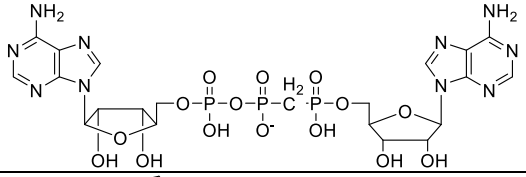
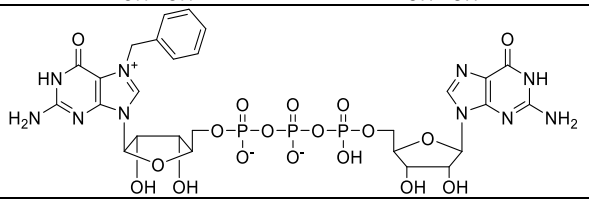
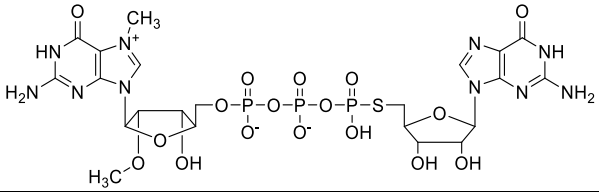
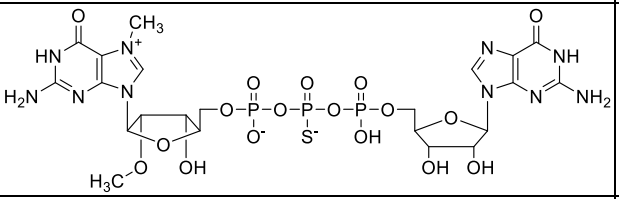
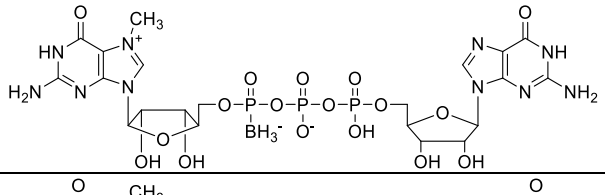
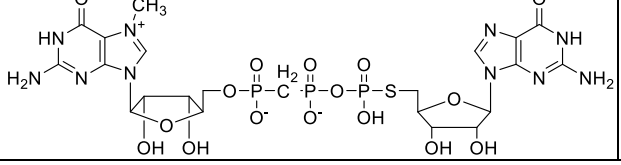
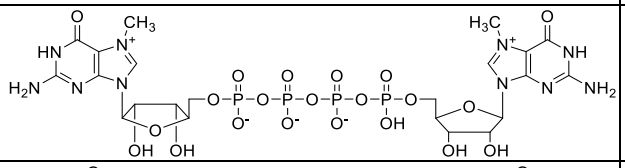
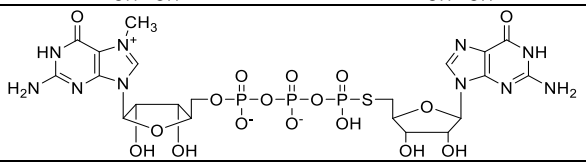
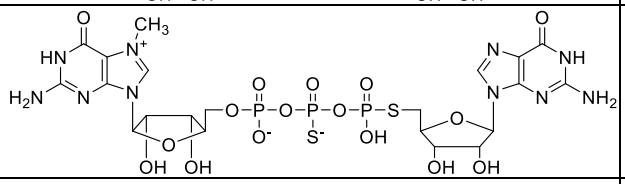
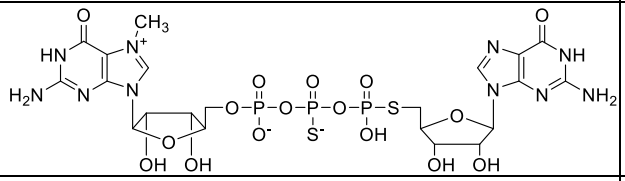
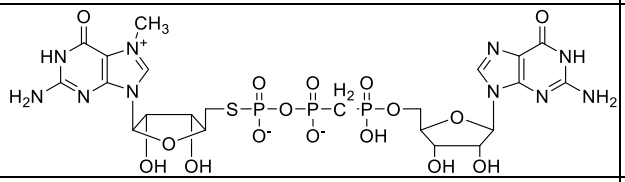
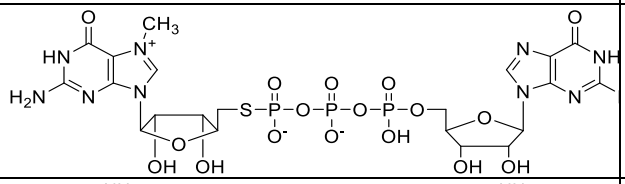
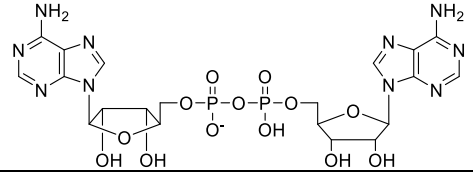
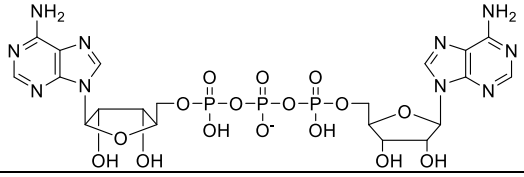
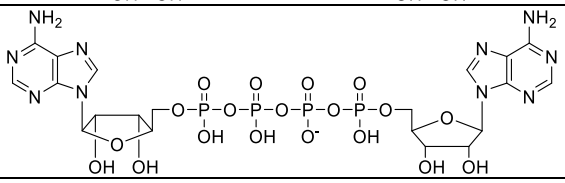
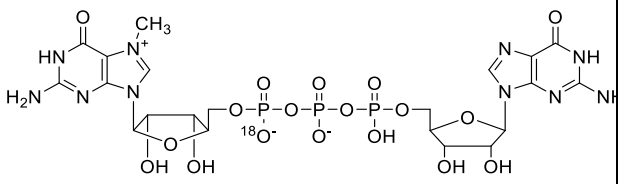
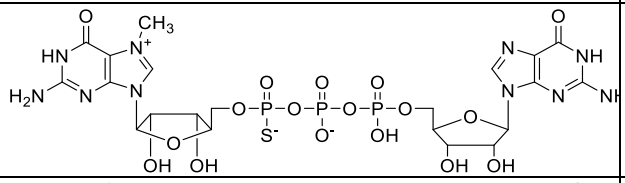
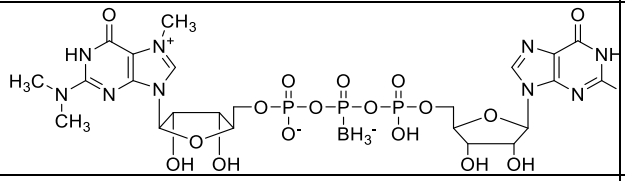
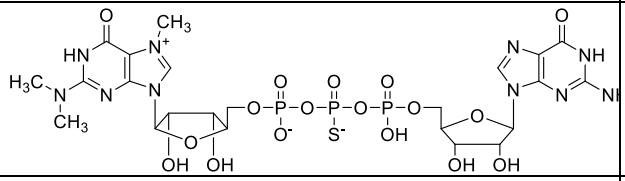
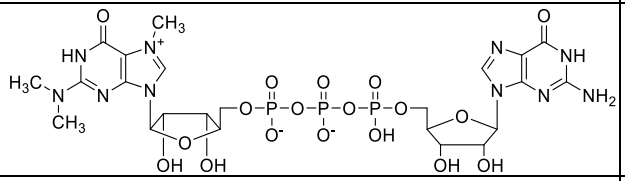
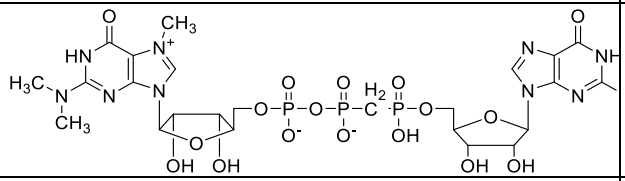
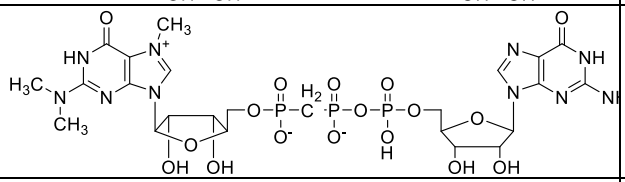
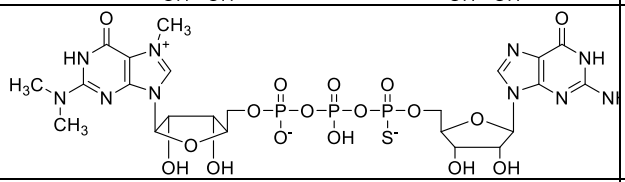
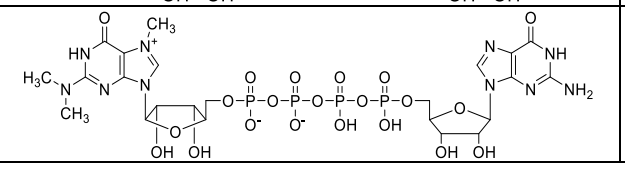


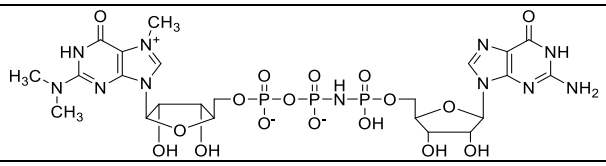
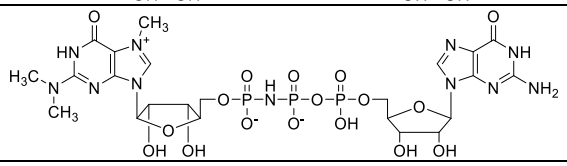
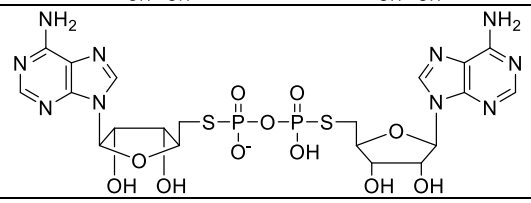
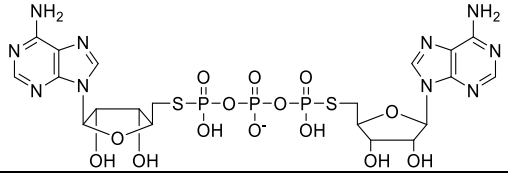
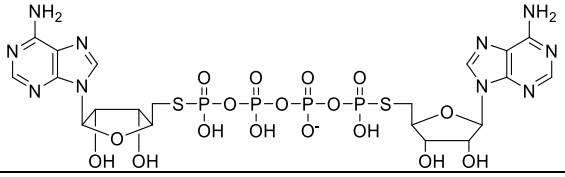
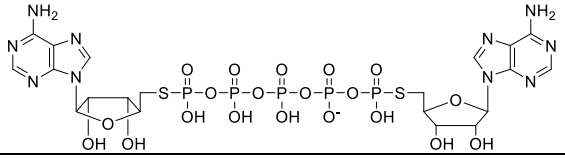
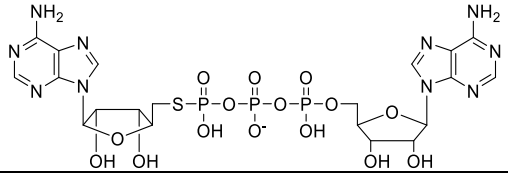
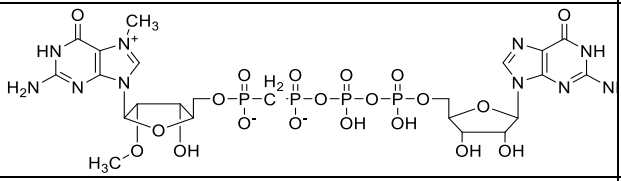
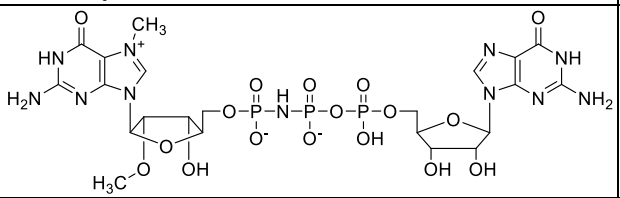
Table S1. Names and structures of investigated compounds. DP and CE values are given in volts. Mass is the nominal mass of the neutral molecule (Da), the observed precursor ions were $[M-H]^-$ and $[M-2H]^{2-}$.

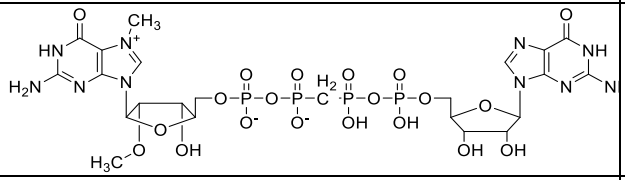
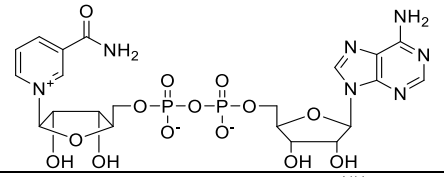
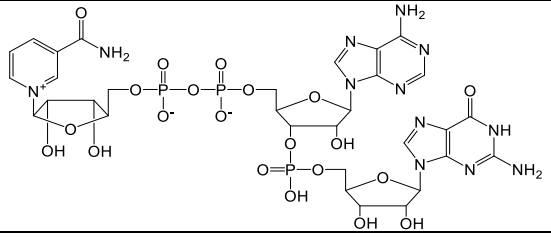
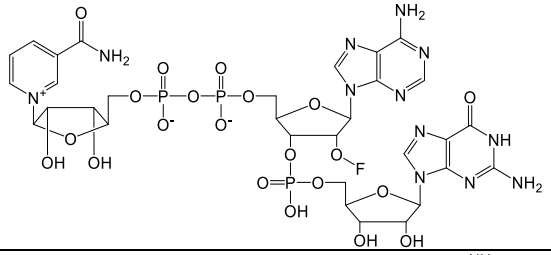
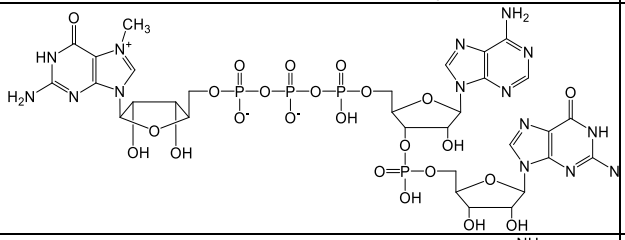
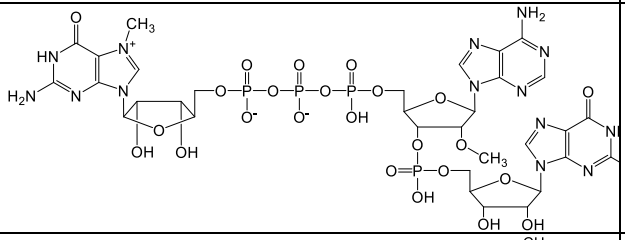
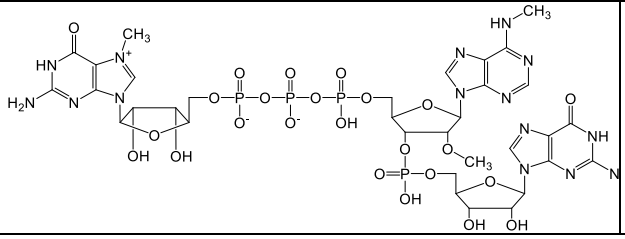
Nr	Abbreviation	Name	Structure	Mass	DP	CE	Ref.[a]
1.	m^7GpppG	guanosine-N^7-methylguanosine 5′,5′-triphosphate		802	-30	-30	[1] (Jemielity et al., 2003)
2.	$GpppA_m$	guanosine-2′-O-methyladenosine 5′,5′-triphosphate		786	-30	-30	[2](Bednarczyk et al.)
3.	$ApppG_m$	adenosine-2′-O-methylguanosine 5′,5′-triphosphate		786	-30	-30	[2](Bednarczyk et al.)
4.	m^7GpppA	adenosine-N^7-methylguanosine 5′,5′-triphosphate		786	-30	-30	[2](Bednarczyk et al.)
5.	m^7Gpppm^6A	N6-methyladenosine-N^7-methylguanosine 5′,5′-triphosphate		800	-30	-30	[2](Bednarczyk et al.)
6.	m^7GpppA_m	2′-O-methyladenosine-N^7-methylguanosine 5′,5′-triphosphate		800	-30	-30	[2](Bednarczyk et al.)
7.	GpppG	diguanosine 5′,5′-triphosphate		788	-30	-40	[2](Bednarczyk et al.)
8.	ApppG	adenosine-guanosine 5′,5′-triphosphate		772	-30	-30	[2](Bednarczyk et al.)
9.	UpppU	diuridine 5′,5′-triphosphate		710	-30	-30	[3](Pietrowska-Borek et al., 2020)

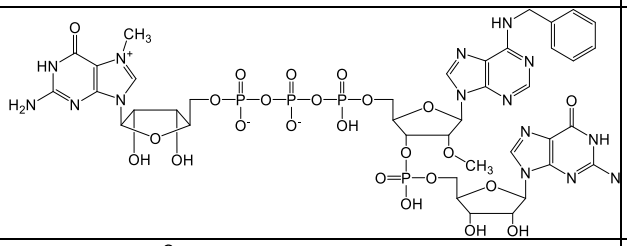
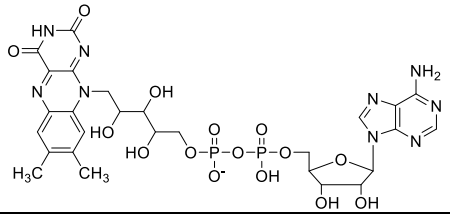
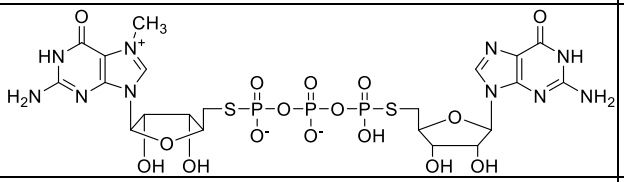
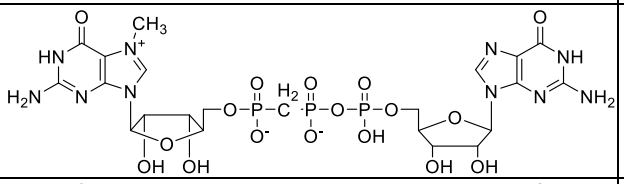
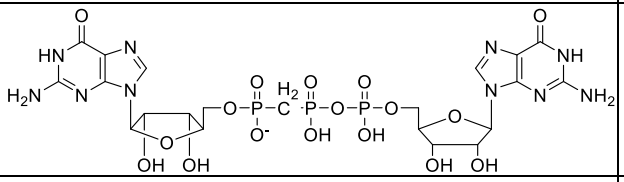
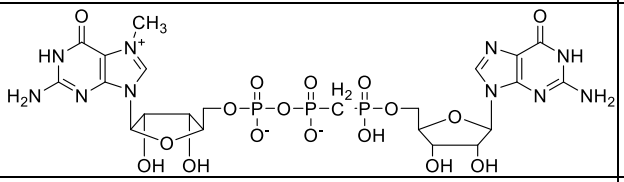
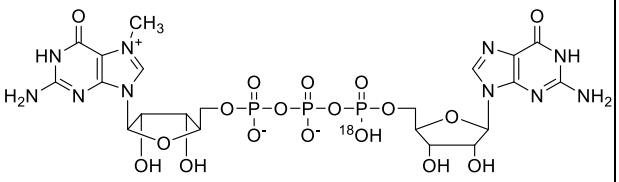
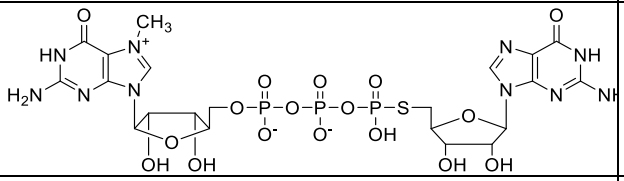
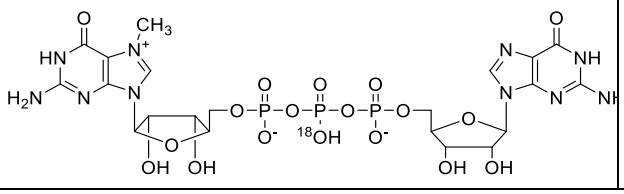
Nr	Abbreviation	Name	Structure	Mass	DP	CE	Ref.[a]
10.	ApppU	adenosine-uridine 5′,5′-triphosphate		733	-30	-30	[3](Pietrowska-Borek et al., 2020)
11.	ApCH$_2$ppU	adenosine-uridine 5′,5′-(1,2-methylene)triphosphate		731	-40	-30	[3](Pietrowska-Borek et al., 2020)
12.	AppCH$_2$pU	adenosine-uridine 5′,5′-(2,3-methylene)triphosphate		731	-40	-30	[3](Pietrowska-Borek et al., 2020)
13.	AppCH$_2$pA	diadenosine 5′,5′-(1,2-methylene)triphosphate		754	-50	-15	[3](Pietrowska-Borek et al., 2020)
14.	Bn^{7}GpppG	N^7-benzylguanosine-guanosine 5′,5′-triphosphate		878	-20	-55	[4](Wojcik et al., 2021)
15.	m^{7,2}OGpppSG	N7,2′-O-dimethylguanosine-5′-thioguanosine 5′,5′-triphosphate		832	-30	-37	[5](Wojtczak et al., 2018)
16.	m^{7,2}OGppSpG	N7,2′-O-dimethylguanosine-guanosine 5′,5′-(2-thio)triphosphate		832	-30	-35	[6](Kowalska et al., 2008)
17.	m^{7}GpBH$_3$ppG	guanosine-N^7-methylguanosine 5′,5′-(3-borano)triphosphate		800	-30	-37	[7](Kowalska et al., 2014)
18.	m^{7}GpCH$_2$ppSG	N^7-methylguanosine-5′-thioguanosine 5′,5′-(1,2-methylene)triphosphate		816	-30	-48	[5](Wojtczak et al., 2018)

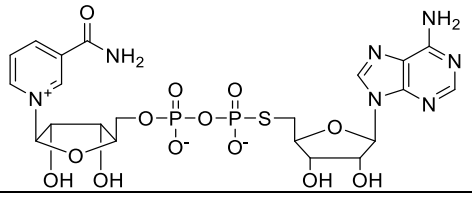
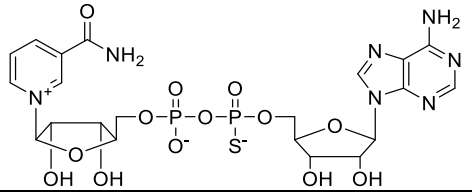
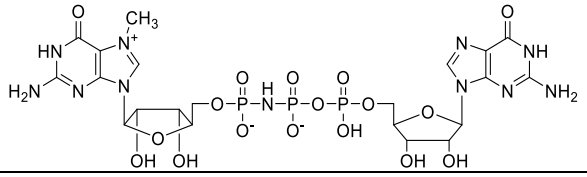
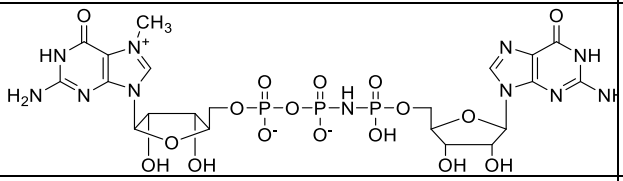
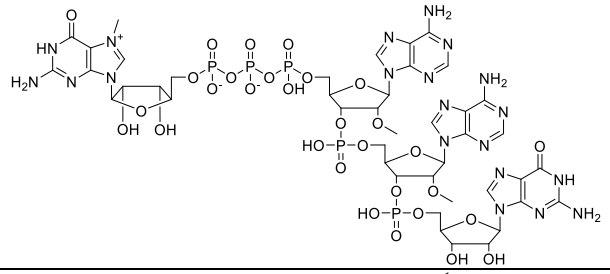
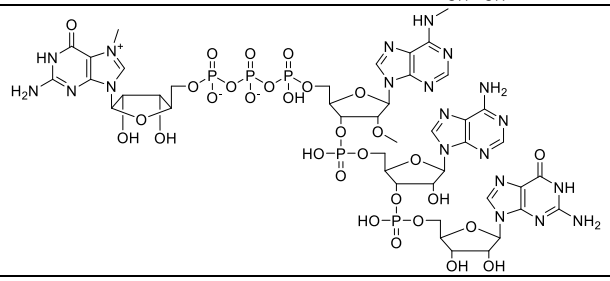
Nr	Abbreviation	Name	Structure	Mass	DP	CE	Ref.[a]
19.	m^7Gpppm^7G	di(N^7-methylguanosine) 5′,5′-tetraphosphate		896	-30	-47	[1](Jemielity et al., 2003)
20.	$m^7GpppSG$	N^7-methylguanosine-5′-thioguanosine 5′,5′-triphosphate		818	-30	-40	[5](Wojtczak et al., 2018)
21.	$m^7GppspSG$ D1	N^7-methylguanosine-5′-thioguanosine 5′,5′-(2-thio)triphosphate (D1 isomer)		834	-40	-30	[5](Wojtczak et al., 2018)
22.	$m^7GppspSG$ D2	N^7-methylguanosine-5′-thioguanosine 5′,5′-(2-thio)triphosphate (D2 isomer)		834	-40	-30	[5](Wojtczak et al., 2018)
23.	$m^7GSppCH_2pG$	N^7-methyl-5′-thioguanosine-guanosine 5′,5′-(1,2-methylene)triphosphate		816	-30	-55	[5](Wojtczak et al., 2018)
24.	$m^7GSpppG$	N^7-methyl-5′-thioguanosine-guanosine 5′,5′-triphosphate		818	-30	-30	[5](Wojtczak et al., 2018)
25.	AppA	diadenosine 5′,5′-diphosphate		676	-30	-55	[3](Pietrowska-Borek et al., 2020)
26.	ApppA	diadenosine 5′,5′-triphosphate		756	-30	-30	[3](Pietrowska-Borek et al., 2020)
27.	AppppA	diadenosine 5′,5′-tetraphosphate		836	-30	-10	[3](Pietrowska-Borek et al., 2020)

Nr	Abbreviation	Name	Structure	Mass	DP	CE	Ref.[a]
28.	$m^7Gp[^{18}O]ppG$	guanosine-N^7-methylguanosine 5′,5′-(3-[^{18}O])triphosphate		804	-30	-41	[8](Strzelecka et al., 2017); [1](Jemielity et al., 2003)
29.	$m^7Gp(s)ppG$	guanosine-N^7-methylguanosine 5′,5′-(3-thio)triphosphate		818	-40	-30	[6](Kowalska et al., 2008)
30.	$TMGpp(BH_3)pG$	guanosine-2,2,7-trimethylguanosine 5′,5′-(2-borano)triphosphate		828	-40	-30	[9](Zytek et al., 2014)
31.	TMGpp(s)pG D2	guanosine-2,2,7-trimethylguanosine 5′,5′-(2-thio)triphosphate (D2 isomer)		847	-40	-30	[9](Zytek et al., 2014)
32.	TMGpppG	guanosine-2,2,7-trimethylguanosine 5′,5′-triphosphate		831	-40	-30	[9](Zytek et al., 2014)
33.	$TMGppCH_2pG$	guanosine-2,2,7-trimethylguanosine 5′,5′-(1,2-methylene)triphosphate		828	-40	-30	[9](Zytek et al., 2014)
34.	$TMGpCH_2ppG$	guanosine-2,2,7-trimethylguanosine 5′,5′-(2,3-methylene)triphosphate		828	-40	-30	[9](Zytek et al., 2014)
35.	TMGppp(s)G	guanosine-2,2,7-trimethylguanosine 5′,5′-(1-thio)triphosphate		847	-40	-30	[9](Zytek et al., 2014)
36.	TMGppppG	guanosine-2,2,7-trimethylguanosine 5′,5′-tetraphosphate		910	-40	-30	[9](Zytek et al., 2014)

Nr	Abbreviation	Name	Structure	Mass	DP	CE	Ref.[a]
37.	TMGppNHpG	guanosine-2,2,7-trimethylguanosine 5′,5′-(1,2-imido)triphosphate		829	-40	-30	[9](Zytek et al., 2014)
38.	TMGpNHppG	guanosine-2,2,7-trimethylguanosine 5′,5′-(2,3-imido)triphosphate		829	-40	-30	[9](Zytek et al., 2014)
39.	ASppSA	di(5′-thioadenosine) 5′,5′-diphosphate		708	-48	-30	[3](Pietrowska-Borek et al., 2020)
40.	ASpppSA	di(5′-thioadenosine) 5′,5′-triphosphate		788	-48	-30	[3](Pietrowska-Borek et al., 2020)
41.	ASppppSA	di(5′-thioadenosine) 5′,5′-tetraphosphate		868	-48	-30	[3](Pietrowska-Borek et al., 2020)
42.	ASpppppSA	di(5′-thioadenosine) 5′,5′-pentaphosphate		948	-40	-30	[3](Pietrowska-Borek et al., 2020)
43.	ASpppA	adenosine-5′-thioadenosine 5′,5′-triphosphate		772	-40	-30	[3](Pietrowska-Borek et al., 2020)
44.	$m^{7,2}OGpCH_2pppG$	N7,2′-O-dimethylguanosine-guanosine 5′,5′-(1,2-methylene)tetraphosphate		894	-40	-55	[10](Kalek et al., 2006)
45.	$m^{7,2}OGpNHppG$	N7,2′-O-dimethylguanosine-guanosine 5′,5′-(2,3-imido)triphosphate		815	-40	-30	[11](Rydzik et al., 2012)

Nr	Abbreviation	Name	Structure	Mass	DP	CE	Ref.[a]
46.	$m^{7,2}OGppCH_2ppG$	N7,2′-O-dimethylguanosine-guanosine 5′,5′-(2,3-methylene)tetraphosphate		894	-40	-30	[12](Rydzik et al., 2009)
47.	NAD	nicotinamide adenine dinucleotide		663	-20	-30	Commercial (Sigma Aldrich)
48.	NADpG	nicotinamide adenine-guanine trinucleotide		1008	-40	-30	[13](Mlynarska-Cieslak et al., 2018)
49.	NAD(F)pG	nicotinamide adenine dinucleotide-2′-fluoroguanosine 5′,5′-phosphate		1010	-30	-25	[13](Mlynarska-Cieslak et al., 2018)
50.	$m^7GpppApG$	N^7-methylguanosine-adenosine-guanosine trinucleotide		1131	-40	-35	[14](Sikorski et al., 2020)
51.	m^7GpppA_mpG	N^7-methylguanosine-2′-O-methyladenosine-guanosine trinucleotide		1145	-45	-60	[14](Sikorski et al., 2020)
52.	$m^7Gpppm^6A_mpG$	N^7-methylguanosine-N^6-methyl-2′-O-methyladenosine-guanosine trinucleotide		1159	-30	-35	[14](Sikorski et al., 2020)

Nr	Abbreviation	Name	Structure	Mass	DP	CE	Ref.[a]
53.	$m^7GpppBn^6A_mpG$	N^7-methylguanosine-N^6-benzyl-2′-O-methyladenosine-guanosine trinucleotide		1235	-30	-35	[15](Warminski et al., 2024)
54.	FAD	flavin adenine dinucleotide		785	-40	-30	[16] (Depaix et al., 2022)
55.	$m^7GSpppSG$	N^7-methyl-5′-thioguanosine-5′-thioguanosine 5′,5′-triphosphate		834	-40	-30	[5](Wojtczak et al., 2018)
56.	m^7GpCH_2ppG	guanosine-N^7-methylguanosine 5′,5′-(2,3-methylene)triphosphate		800	-40	-30	[10](Kalek et al., 2006)
57.	$GpCH_2ppG$	diguanosine 5′,5′-(1,2-methylene)triphosphate		786	-100	-30	[3](Pietrowska-Borek et al., 2020)
58.	m^7GppCH_2pG	guanosine-N7-methylguanosine 5′,5′-(1,2-methylene)triphosphate		800	-100	-30	[10](Kalek et al., 2006)
59.	$m^7Gppp[^{18}O]G$	guanosine-N^7-methylguanosine 5′,5′-(1-[^{18}O])triphosphate		804	-100	-30	[8](Strzelecka et al., 2017); [1](Jemielity et al., 2003)
60.	$m^7Gppp(s)G$	guanosine-N^7-methylguanosine 5′,5′-(1-thio)triphosphate		818	-100	-30	[5](Wojtczak et al., 2018)
61.	$m^7Gpp[^{18}O]pG$	guanosine-N7-methylguanosine 5′,5′-(2-[^{18}O])triphosphate		804	-40	-30	[8](Strzelecka et al., 2017); [1](Jemielity et al., 2003)

Nr	Abbreviation	Name	Structure	Mass	DP	CE	Ref.[a]
62.	NAD5'S	nicotinamideriboside 5'-thioadenosine 5',5'-diphosphate		679	-20	-30	[13](Mlynarska-Cieslak et al., 2018)
63.	NADαS	adenosine nicotinamideriboside 5',5'-(1-thio)diphosphate		679	-20	-30	[13](Mlynarska-Cieslak et al., 2018)
64.	m^7GpNHppG	guanosine-N7-methylguanosine 5′,5′-(2,3-imido)triphosphate		801	-40	-44	[11](Rydzik et al., 2012)
65.	m^7GppNHpG	guanosine-N7-methylguanosine 5′,5′-(1,2-imido)triphosphate		801	-40	-30	[11](Rydzik et al., 2012)
66.	m^7GpppA$_m$pA$_m$pG	N7-methylguanosine-2′-O-methyladenosine-2′-O-methyladenosine-guanosine tetranucleotide		1488	-50	-45	[2](Bednarczyk et al.)
67.	m^7Gppp m^6A_mpApG	N7-methylguanosine-N6-methyl-2′-O-methyladenosine-adenosine-guanosine tetranucleotide		1488	-50	-45	[2](Bednarczyk et al.)

1 Jemielity, J. *et al.* Novel "anti-reverse" cap analogs with superior translational properties. *RNA* **9**, 1108-1122, doi:10.1261/rna.5430403 (2003).

2 Bednarczyk et al. under preparation.

3 Pietrowska-Borek, M. *et al.* Purine and pyrimidine dinucleoside polyphosphates differentially affect the phenylpropanoid pathway in Vitis vinifera L. cv. Monastrell suspension cultured cells. *Plant Physiol. Biochem.* **147**, 125-132, doi:10.1016/j.plaphy.2019.12.015 (2020).

4 Wojcik, R. *et al.* Novel N7-arylmethyl substituted dinucleotide mRNA 5′ cap analogs: synthesis and evaluation as modulators of translation. *Pharmaceutics* **13**, 1941, doi:10.3390/pharmaceutics13111941 (2021).

5 Wojtczak, B. *et al.* 5′-phosphorothiolate dinucleotide cap analogues: reagents for messenger RNA modification and potent small-molecular inhibitors of decapping enzymes. *J. Am. Chem. Soc.* **140**, 5987-5999, doi:10.1021/jacs.8b02597 (2018).

6 Kowalska, J. *et al.* Synthesis and characterization of mRNA cap analogs containing phosphorothioate substitutions that bind tightly to eIF4E and are resistant to the decapping pyrophosphatase DcpS. *RNA* **14**, 1119-1131, doi:10.1261/rna.990208 (2008).

7 Kowalska, J. *et al.* Synthesis, properties, and biological activity of boranophosphate analogs of the mRNA cap: versatile tools for manipulation of therapeutically relevant cap-dependent processes. *Nucleic Acids Res.* **42**, 10245-10264, doi:10.1093/nar/gku757 (2014).

8 Strzelecka, D., Chmielinski, S., Bednarek, S., Jemielity, J. & Kowalska, J. Analysis of mononucleotides by tandem mass spectrometry: investigation of fragmentation pathways for phosphate- and ribose-modified nucleotide analogues. *Sci. Rep.* **7**, 8931, doi:10.1038/s41598-017-09416-6 (2017).

9 Zytek, M. *et al.* Towards novel efficient and stable nuclear import signals: synthesis and properties of trimethylguanosine cap analogs modified within the 5′,5′-triphosphate bridge. *Org. Biomol. Chem.* **12**, 9184-9199, doi:10.1039/c4ob01579g (2014).

10 Kalek, M. *et al.* Enzymatically stable 5′ mRNA cap analogs: Synthesis and binding studies with human DcpS decapping enzyme. *Bioorg. Med. Chem.* **14**, 3223-3230, doi:10.1016/j.bmc.2005.12.045 (2006).

11 Rydzik, A. *et al.* Synthesis and properties of mRNA cap analogs containing imidodiphosphate moiety-fairly mimicking natural cap structure, yet resistant to enzymatic hydrolysis. *Bioorg. Med. Chem.* **20**, 1699-1710, doi:10.1016/j.bmc.2012.01.013 (2012).

12 Rydzik, A. *et al.* Synthetic dinucleotide mRNA cap analogs with tetraphosphate 5′,5′ bridge containing methylenebis(phosphonate) modification. *Org. Biomol. Chem.* **7**, 4763-4776, doi:10.1039/b911347a (2009).

13 Mlynarska-Cieslak, A. *et al.* Nicotinamide-containing di- and trinucleotides as chemical tools for studies of NAD-capped RNAs. *Org. Lett.* **20**, 7650-7655, doi:10.1021/acs.orglett.8b03386 (2018).

14 Sikorski, P. *et al.* The identity and methylation status of the first transcribed nucleotide in eukaryotic mRNA 5′ cap modulates protein expression in living cells. *Nucleic Acids Res.* **48**, 1607-1626, doi:10.1093/nar/gkaa032 (2020).

15 Warminski, M. *et al.* Trinucleotide mRNA cap analogue N6-benzylated at the site of posttranscriptional $^{m6}A_m$ mark facilitates mRNA purification and confers superior translational properties in vitro and in vivo. *J. Am. Chem. Soc.* **146**, 8149-8163, doi:10.1021/jacs.3c12629 (2024).

16 Depaix, A. *et al.* Preparation of RNAs with non-canonical 5' ends using novel di- and trinucleotide reagents for co-transcriptional capping. *Front. Mol. Biosci.* **9**, 854170, doi:10.3389/fmolb.2022.854170 (2022).

Table S2. Characteristic fragment-ion types observed for mono- and dinucleotide analogs

Fragments Type	Mononucleotides	Dinucleotides
Phosphate	✓	✓
Nucleobase	✓	✓
Ribose-phosphate	✓	✓
Nucleotide	✓	✓
Ribose-nucleotide	–	✓

Table S3. Comparison of MS/MS fragment ions of m^7GpppG and positionally ^{18}O-labeled analogues.

Fragments Type	m^7GpppG	m^7Gp[^{18}O]ppG	m^7Gpp[^{18}O]pG	m^7Gppp[^{18}O]G
	m/z (Structural Assignment)			
Phosphate	159 (HP_2O_6), 177 ($H_2P_2O_7$)	161 ([^{18}O]-HP_2O_6), 179 ([^{18}O]-$H_2P_2O_7$)	161 ([^{18}O]-HP_2O_6), 179 ([^{18}O]-$H_2P_2O_7$)	161 ([^{18}O]-HP_2O_6), 179 ([^{18}O]-$H_2P_2O_7$)
Ribose-phosphate	273 (Rpp-H_2O), 353 (Rppp-H_2O)	275 ([^{18}O]-Rpp-H_2O), 355 ([^{18}O]-Rppp-H_2O)	275 ([^{18}O]-Rpp-H_2O), 355 ([^{18}O]-Rppp-H_2O)	275 ([^{18}O]-Rpp-H_2O), 355 ([^{18}O]-Rppp-H_2O)
Nucleotide diphosphate (G-derived)	424 (Gpp-H_2O), 442 (Gpp)	426 ([^{18}O]-Gpp-H_2O), 444 ([^{18}O]-Gpp)	426 ([^{18}O]-Gpp-H_2O), 444 ([^{18}O]-Gpp)	426 ([^{18}O]-Gpp-H_2O), 444 ([^{18}O]-Gpp)
Nucleotide diphosphate (m^7G-derived)	438 (m^7Gpp-H_2O), 456 (m^7Gpp)	440 ([^{18}O]-m^7Gpp-H_2O), 458 ([^{18}O]-m^7Gpp)	440 ([^{18}O]-m^7Gpp-H_2O), 458 ([^{18}O]-m^7Gpp)	440 ([^{18}O]-m^7Gpp-H_2O), 458 ([^{18}O]-m^7Gpp)
Nucleotide triphosphate	504 (Gppp-H_2O)	506 ([^{18}O]-Gppp-H_2O)	506 ([^{18}O]-Gppp-H_2O)	506 ([^{18}O]-Gppp-H_2O)
Ribose-nucleotide	636 (GpppR)	638 ([^{18}O]-GpppR)	638 ([^{18}O]-GpppR)	638 ([^{18}O]-GpppR)

Note: Only selected isotope-shifted fragment ions are listed for the labeled compounds. Unshifted counterparts were also observed in the corresponding MS/MS spectra (Supplementary Fig. S1). The notation [^{18}O] indicates the presence of one ^{18}O atom without specifying its position within the fragment structure.

Table S4. Comparison of MS/MS fragment ions of ApppA, ApppU and ApppG

Fragments Type	ApppA	ApppU	ApppG
	m/z (Structural Assignment)		
Nucleobase	134 (A)	134 (A)/ 111 (U)	134 (A)/ 150 (G)
Nucleotide monophosphate	346(Ap), 328 (Ap-H_2O)	346(Ap), 328 (Ap-H_2O)/ 323 (Up), 305 (Up-H_2O)	346(Ap), 328 (Ap-H_2O)/ 362 (Gp), 344 (Gp-H_2O)
Nucleotide diphosphate	426 (App), 408 (App-H_2O)	426 (App), 408 (App-H_2O)/ 403 (Upp), 385 (Upp-H_2O)	426 (App), 408 (App-H_2O)/ 442 (Gpp), 424 (Gpp-H_2O)
Nucleotide triphosphate	488 (Appp-H_2O)	488 (Appp-H_2O)/ 465 (Uppp-H_2O)	488 (Appp-H_2O)/ 504 (Gppp-H_2O)

Table S5. Comparison of MS/MS fragment ions of AppA, ApppA and AppppA

Fragments Type	AppA	ApppA	AppppA
	m/z (Structural Assignment)		
Nucleotide monophosphate	328 (Ap-H_2O)	328 (Ap-H_2O)	-
	346 (Ap)	-	-
Nucleotide diphosphate	408 (App-H_2O)	408 (App-H_2O)	408 (App-H_2O)
	426 (App)	426 (App)	426 (App)
Nucleotide triphosphate	-	488 (Appp-H_2O)	488 (Appp-H_2O)
	-	-	506 (Appp)

Table S6. Comparison of MS/MS fragment ions of ASppSA, ASpppSA, ASppppSA and ASpppppSA

Fragments Type	ASppSA	ASpppSA	ASppppSA	ASpppppSA
	m/z (Structural Assignment)			
Nucleotide monophosphate	344 (ASp-H_2O)	344 (ASp-H_2O)	344 (ASp-H_2O)	-
	362 (ASp)	-	-	-
Nucleotide diphosphate	424 (ASpp-H_2O)	424 (ASpp-H_2O)	424 (ASpp-H_2O)	424 (ASpp-H_2O)
	-	442 (ASpp)	442 (ASpp)	-
Nucleotide triphosphate	-	504 (ASppp-H_2O)	504 (ASppp-H_2O)	504 (ASppp-H_2O)
	-	-	522 (ASppp)	-
Nucleotide tetraphosphate	-	-	584 (ASpppp-H_2O)	584 (ASpppp-H_2O)
	-	-	-	602 (ASpppp)

Table S7. Comparison of MS/MS fragment ions of $GpppA_m$, m^7GpppA and $ApppG_m$

Fragments Type	$GpppA_m$	m^7GpppA	$ApppG_m$
	m/z (Structural Assignment)		
Nucleobase	-	164 (m^7G)	-
Ribose-phosphate	273 (Rpp-H_2O), 287 ($R_m$pp-H_2O)	273 (Rpp-H_2O)	273 (Rpp-H_2O), 287 ($R_m$pp-H_2O)
Nucleotide monophosphate	360 (A_mp)	376 (m^7Gp)	376 (G_mp), 358 (G_mp-H_2O)
Nucleotide diphosphate	422 ($A_m$pp-H_2O), 440 ($A_m$pp)	438 (m^7Gpp-H_2O)	438 ($G_m$pp-H_2O), 456 ($G_m$pp)
Nucleotide triphosphate	-	-	518 ($G_m$ppp-H_2O)

Table S8. Comparison of MS/MS fragment ions of m^7GpppA_m and m^7Gpppm^6A

Fragments Type	m^7GpppA_m	m^7Gpppm^6A
	m/z (Structural Assignment)	
Nucleobase	134 (A)	148 (m^6A)
Ribose-phosphate	273 (Rpp-H_2O), 287 ($R_m$pp-H_2O)	273 (Rpp-H_2O)
Nucleotide monophosphate	360 (A_mp)	342 (m^6Ap-H_2O), 360 (m^6Ap)
Nucleotide diphosphate	422 ($A_m$pp-H_2O)	422 (m^6App-H_2O)
Nucleotide triphosphate	502 ($A_m$ppp-H_2O)	502 (m^6Appp-H_2O)

Table S9. Characteristic fragment-ion types observed for di- and trinucleotide analogs

Fragments Type	Dinucleotides	Trinucleotides
Phosphate	✓	✓
Nucleobase	✓	✓
Ribose-phosphate	✓	✓
Nucleotide	✓	✓
Ribose-nucleotide	✓	✓
Dinucleotide-derived	–	✓
Ribose-dinucleotide	–	✓

Table S10. Comparison of MS/MS fragment ions of $m^7GpppXpG$ (where X=A_m, m^6A_m, Bn^6A_m) trinucleotide derivatives.

Fragments Type	Structural Assignment	m^7GpppA_mpG	$m^7Gpppm^6A_mpG$	$m^7GpppBn^6A_mpG$
		m/z values		
Nucleotide diphosphate	ppX-H_2O	422	436	512
Nucleotide triphosphate	pppX-H_2O	502	516	592
Dinucleotide monophosphate	pXpG-H_2O	687	701	777
	pXpG	705	719	795
Dinucleotide diphosphate	ppXpG-H_2O	767	781	857
	ppXpG	785	799	875
Dinucleotide triphosphate	pppXpG-H_2O	847	861	937
	pppXpG	865	879	955
Ribose-dinucleotide	RpppXpG-H_2O	961	975	1051
	RpppXpG	979	993	1069

Note: Substitution of m^6A_m results in a +14 Da shift corresponding to the methyl group relative to A_m. Bn^6A_m produces a +90 Da shift relative to A_m corresponding to the benzyl group. Most fragments appear as pairs representing intact ions and dehydration products (-H_2O)

Table S11. Comparison of diagnostic MS/MS fragment ions of isomeric mRNA cap analogs Cap 2, m^6A-Cap 1, and their mixture.

Fragments Type	Cap 2 ($m^7GpppA_mpA_mpG$)	m^6A-Cap 1 ($m^7Gpppm^6A_mpApG$)	Mixture
	m/z values		
Nucleotide diphosphate	422 (A_mpp-H_2O)	-	422 (A_mpp-H_2O)
Nucleotide diphosphate	-	436 (m^6A_mpp-H_2O)	436 (m^6Ampp-H_2O)
Nucleotide triphosphate	502 (A_mppp-H_2O)	-	<1%
Nucleotide triphosphate	-	516 (m^6A_mppp-H_2O)	<1%